

Hairy and enhancer of split 1 (HES1) protects cells from endoplasmic reticulum stress–induced apoptosis through repression of *GADD34*

Received for publication, January 26, 2018, and in revised form, February 26, 2018. Published, Papers in Press, February 28, 2018, DOI 10.1074/jbc.RA118.002124

Ji Eun Lee¹, William Morrison², and Julie Hollien³

From the Department of Biology and the Center for Cell and Genome Science, University of Utah, Salt Lake City, Utah 84112

Edited by Ronald C. Wek

Disruption in endoplasmic reticulum (ER) function, termed ER stress, occurs in many diseases, including neurodegenerative disorders, diabetes, and cancer. Cells respond to ER stress with the unfolded protein response (UPR), which triggers a broad transcriptional program to restore and enhance ER function. Here, we found that ER stress up-regulates the mRNA encoding the developmentally regulated transcriptional repressor hairy and enhancer of split 1 (*HES1*), in a variety of cell types. Depletion of *HES1* increased cell death in response to ER stress in mouse and human cells, in a manner that depended on the pro-apoptotic gene growth arrest and DNA damage-inducible protein *GADD34* (also known as *Protein phosphatase 1 regulatory subunit 15A*, or *MyD116*). Furthermore, *HES1* bound to the *GADD34* promoter, and its depletion led to an up-regulation of *GADD34* expression during ER stress. Our results identify *HES1* as a repressor of *GADD34* expression, and reveal that *HES1* contributes to cell fate determination in response to ER stress.

As a central organelle in the protein secretory pathway, the endoplasmic reticulum (ER)⁴ is responsible for folding and processing secreted and membrane proteins. Alterations in ER function can arise from various stimuli such as increased secretory protein synthesis during the differentiation of secretory cells, or diseases that disrupt the function of protein folding pathways. These perturbations lead to an imbalance between the load and capacity of the ER, referred to as ER stress. To avoid or counteract the potentially toxic accumulation of misfolded proteins, the ER responds to stress through the unfolded

protein response (UPR) (1). This collection of signaling pathways relieves the protein-folding load on the ER by global translational attenuation and mRNA decay (2, 3), while simultaneously increasing the ability of the ER to fold proteins by up-regulation of genes encoding ER-specific chaperones (1).

The UPR is initiated by three ER membrane-embedded signaling proteins: PKR-like ER kinase (PERK), inositol-requiring enzyme 1 (IRE1), and activating transcription factor 6 (ATF6). Translational regulation is mediated by PERK, which phosphorylates eukaryotic translation initiation factor 2 α (eIF2 α) (2). This inhibits general translation but promotes synthesis of proteins such as ATF4, whose mRNAs contain upstream open reading frames (4). ATF4 subsequently activates transcription of ER chaperones and genes involved in amino acid metabolism and antioxidant pathways, which are required for ER quality control (5). A second transducer of the UPR is IRE1, whose endoribonuclease is activated by ER stress. IRE1 mediates the unconventional splicing of the mRNA encoding the transcription factor X-box-binding protein 1 (*XBP1*) (6), thereby increasing expression of many genes encoding ER chaperones and other proteins that function in the secretory pathway (7). IRE1 also cleaves other mRNAs localized to the ER, leading to their degradation through regulated IRE1-dependent decay (RIDD) (8). ATF6 is activated by proteolysis during ER stress and, along with ATF4 and *XBP1*, up-regulates genes necessary to reestablish protein homeostasis (9).

In addition to its cytoprotective roles, the UPR induces apoptotic cell death if the stress is not mitigated (10). IRE1 recruits TNF receptor-associated factor 2 (TRAF2), which interacts with apoptotic-signaling kinase-1 (ASK1) (1, 11), triggering kinase cascades that promote apoptosis (12, 13). The PERK–ATF4 branch up-regulates a pro-apoptotic transcription factor, C/EBP homologous protein (CHOP), causing changes in gene expression that favor apoptosis (14, 15). For example, CHOP-mediated up-regulation of *GADD34* enhances dephosphorylation of eIF2 α , reversing translational attenuation, which further increases the protein-folding burden on the ER (16). Although many studies have uncovered molecules involved in the ER stress–related apoptosis pathway, it is still unclear how the numerous signals from the stressed ER are integrated and how cells decide to activate apoptosis.

Here we report a novel role for hairy and enhancer of split 1 (*HES1*) in cell fate decisions during ER stress. *HES1* is a basic helix-loop-helix transcriptional repressor (17). As a primary target of the Notch signaling pathway, *HES1* regulates cell qu-

This work was supported in part by General Medical Science Institute, National Institutes of Health Grant R35 GM119540. The authors declare that they have no conflicts of interest with the contents of this article. The content is solely the responsibility of the authors and does not necessarily represent the official views of the National Institutes of Health.

¹ Present address: Cancer Biology and Genetics Program, Memorial Sloan Kettering Cancer Center, New York, NY.

² Present address: Recursion Pharmaceuticals, Salt Lake City, UT.

³ To whom correspondence should be addressed. Tel.: 801-587-7783; E-mail: hollien@biology.utah.edu.

⁴ The abbreviations used are: ER, endoplasmic reticulum; UPR, unfolded protein response; PERK, PKR-like ER kinase; IRE1, inositol-requiring enzyme 1; ATF6, activating transcription factor 6; eIF2 α , eukaryotic translation initiation factor 2 α ; *XBP1*, X-box-binding protein 1; CHOP, C/EBP homologous protein; *HES1*, hairy and enhancer of split 1; Tg, thapsigargin; qPCR, quantitative PCR; ISRIB, integrated stress response inhibitor; CHX, cycloheximide; PI, propidium iodide; BisTris, 2-[bis(2-hydroxyethyl)amino]-2-(hydroxymethyl)propane-1,3-diol; *GADD34*, growth arrest and DNA damage-inducible protein 34.

HES1 regulates GADD34 during ER stress

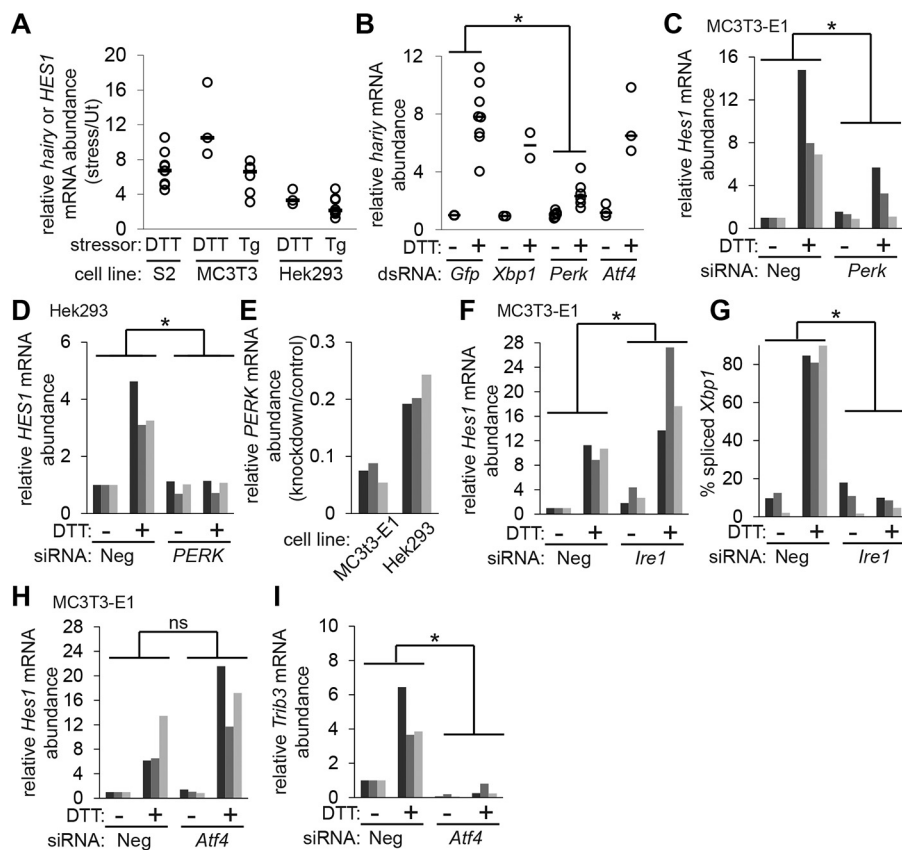


Figure 1. Up-regulation of hairy/HES1 mRNA during ER stress depends on PERK. *A*, we treated *D. melanogaster* S2 cells with DTT (2 mM, 2.5 h), and mouse MC3T3-E1 and human Hek293 cells with either DTT (2 mM, 5 h) or Tg (2 μ M, 2 h) to induce ER stress, and measured relative hairy/HES1 mRNA levels. *Ut*, untreated. *B*, we used RNAi to deplete S2 cells of the indicated UPR transducers (or as a control, GFP), then incubated cells with and without DTT (2 mM, 2.5 h), and measured hairy mRNA levels. Target mRNAs were each significantly depleted (p value < 0.05, paired t test) to an average of 22%, as determined by qPCR. *C–E*, we transfected MC3T3-E1 or Hek293 cells with either control (Neg) or PERK siRNAs and then incubated with or without DTT for 4 h. The colors for the knockdown controls in *E* are matched with the Hes1 measurements in *C* or *D*. *F–I*, we transfected MC3T3-E1 cells with control (Neg), *Ire1*, or *Atf4* siRNAs and then incubated with or without DTT for 4 h. As knockdown controls, we measured Xbp1 splicing in *Ire1*-depleted cells (*G*) by amplifying around the splice site and running the products on a gel, and measured the ATF4 target gene *Trib3* in *Atf4*-depleted cells (*I*). The colors of bars representing individual replicate experiments are maintained across panels in *F–I*. For all panels (except *G*), we measured relative mRNA abundances by qPCR and normalized to the housekeeping control *Rpl19*. In *A* and *B*, short lines indicate the median of replicate experiments. For all figures, markers and bars represent individual experiments. Bars of the same color in each panel indicate treatments done in parallel. *, p value < 0.05, paired two-tailed Student's t test on \log_2 -transformed data to test for fold-changes (stressed/unstressed).

escence and proliferation in the development of multiple organs and cell types (18). HES1 mRNA levels have been reported to increase during ER stress in mouse cells (19), although the mechanism of this regulation has not been previously explored. Here we show that HES1 mRNA levels increase in a manner that depends on the ability of PERK to attenuate translation, and affects the survival of cells exposed to chemical inducers of ER stress by repressing GADD34.

Results

Hairy/HES1 mRNA levels increase during ER stress

To measure the response of HES1 to ER stress, we treated *Drosophila melanogaster* S2, mouse MC3T3-E1, and human HEK293 cells with either dithiothreitol (DTT), a reducing agent that disrupts disulfide bonds, or thapsigargin (Tg), which depletes ER calcium reserves. We then measured relative mRNA levels of fly hairy, or mammalian HES1 by quantitative real-time RT-PCR (qPCR). We found that hairy/HES1 mRNA levels increased during ER stress in all three cell lines (Fig. 1A).

HES1 mRNA up-regulation depends on PERK-mediated translational attenuation

To determine which branch of the UPR signaling network is responsible for the up-regulation of hairy/HES1 mRNA during ER stress, we depleted UPR transducers from S2 cells using RNAi, then compared the mRNA levels of hairy in cells treated with and without DTT for 2.5 h (the time of maximal hairy induction in these cells). Depletion of *Perk*, but not its downstream target *Atf4*, resulted in loss of hairy mRNA up-regulation (Fig. 1B). To test whether mammalian PERK is necessary for HES1 mRNA up-regulation, we transfected MC3T3-E1 or Hek293 cells with siRNAs targeting either PERK or a negative control sequence (Neg), and induced ER stress with DTT. Induction of HES1 mRNA was significantly blocked by PERK knockdown (Fig. 1, C–E).

In contrast to *Perk* knockdown, depletion of *Ire1* in MC3T3-E1 cells resulted in increased induction of the Hes1 mRNA during stress (Fig. 1F). We have not explored the reason for this, but speculate that knockdown of *Ire1* may exacerbate

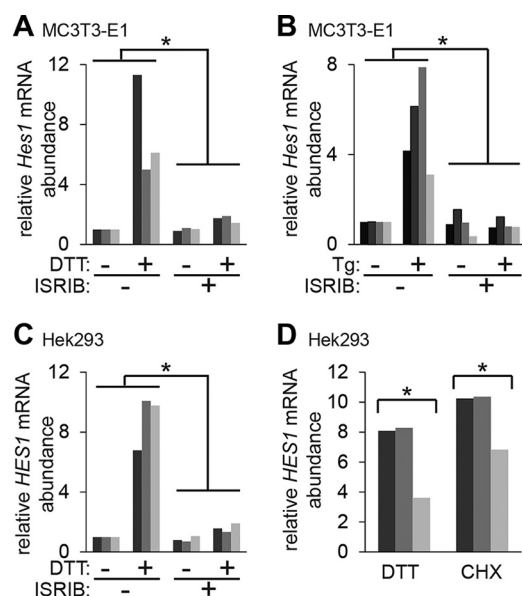


Figure 2. Translational attenuation mediated by PERK is required for *HES1* up-regulation. *A* and *B*, we treated MC3T3-E1 cells with the indicated compounds for 4 h (2 mM DTT) or 2 h (2 μ M Tg). *C*, we treated Hek2993 cells with the indicated compounds for 2 h. *D*, we treated Hek2993 cells with either 35 μ M CHX or 2 mM DTT for 4 h. For all panels, we measured mRNA levels by qPCR. *, *p* value <0.05, paired two-tailed Student's *t* test on log₂-transformed data to test for fold-changes (stressed/unstressed). In *D*, * indicates a comparison between DTT- or CHX-treated to untreated conditions.

ER stress, leading to enhanced PERK signaling and therefore higher *Hes1* mRNA levels. Splicing of *Xbp1* served as a control for *Ire1* knockdown efficiency (Fig. 1*G*). Depletion of *Atf4* did not have significant effects on *Hes1* mRNA levels, although it did block induction of its target gene *Trib3* as expected (Fig. 1, *H* and *I*). These results indicate a conserved effect of PERK, but not ATF4, on *HES1* mRNA up-regulation across cells from flies, mice, and humans.

PERK phosphorylates the translation initiation factor eIF2 α , as well as other targets such as NRF2 (20), diacylglycerol (21), and FOXO1 (22). To determine which aspect of PERK function is important for *HES1* mRNA regulation, we used integrated stress response inhibitor (ISRIB), a small molecule that blocks translational attenuation upon ER stress by inhibiting the downstream effects of eIF2 α phosphorylation (23). ISRIB reduced *HES1* mRNA levels induced by either DTT or Tg treatment in MC3T3-E1 (Fig. 2, *A* and *B*) and Hek2993 cells (Fig. 2*C*), indicating that the translational attenuation mediated by PERK is important for *HES1* regulation. Translational attenuation was also sufficient to increase *HES1* mRNA levels, as seen when we treated cells with the translation elongation inhibitor cycloheximide (CHX) (Fig. 2*D*).

HES1 is known to repress its own expression by directly binding to N-box sequences in its promoter (24). The *HES1* protein and *HES1* mRNA are also highly unstable, and thus their levels would potentially be very sensitive to acute changes in translation and transcription (25). The observation that translation attenuation is both necessary (during ER stress) and sufficient for up-regulation of *HES1* mRNA suggested that increased expression of *HES1* mRNA may be a direct consequence of the loss of *HES1* protein. To address this possibility, we first monitored *HES1* protein (Fig. 3, *A* and *B*) and mRNA

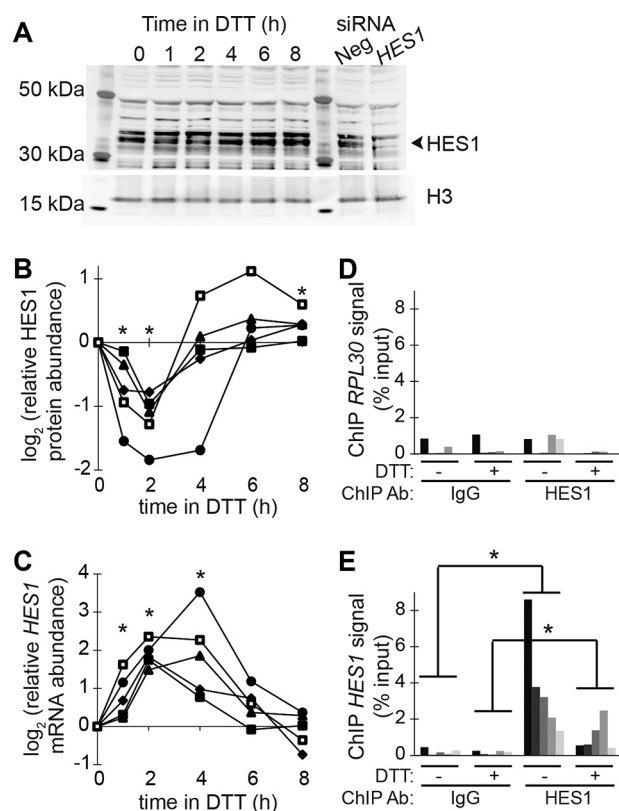


Figure 3. Negative autoregulation of *HES1* during ER stress. *A–C*, we treated Hek2993 cells with DTT (2 mM) and collected whole cell lysates and RNA samples over time. We measured *HES1* protein levels by Western blotting of lysates (*A* and *B*) and *HES1* mRNA levels by qPCR (*C*). For *B* and *C*, symbols representing individual replicate experiments are correlated; protein and mRNA samples collected in parallel are represented by the same symbols in *B* and *C*. *D* and *E*, we treated Hek2993 cells with or without DTT (2 mM, 4 h), cross-linked, and immunoprecipitated endogenous *HES1*, using an IgG antibody as a control in parallel. We then measured the relative abundance of the *HES1* promoter region (*E*) in the precipitated chromatin by qPCR with *RPL30* exon3 as a negative control (*D*). The colors of bars representing individual replicate experiments are maintained across panels *D* and *E*. *, *p* value <0.05, paired two-tailed Student's *t* test on log₂-transformed data to test for fold-changes.

(Fig. 3*C*) levels over time in Hek2993 cells treated with DTT. *HES1* protein levels rapidly declined with DTT, then began to recover after ~2 h (Fig. 3*B*). In contrast, *HES1* mRNA levels increased in the presence of DTT until 2–4 h and then returned to normal levels by 6–8 h (Fig. 3*C*). We carried out five replicates of these time course experiments. In one of the replicates (circles), the *HES1* protein was down-regulated more strongly and for ~2 h longer (Fig. 3*B*); in this same replicate, the *HES1* mRNA continued its upward trajectory for 2 h longer before returning to baseline (Fig. 3*C*). These data are consistent with a negative autoregulation model, where the *HES1* protein controls expression of its own mRNA.

We next asked whether *HES1* is released from its own promoter during ER stress (Fig. 3, *D* and *E*). Chromatin immunoprecipitation (ChIP) analysis revealed robust binding of the endogenous *HES1* protein to the *HES1* promoter in unstressed Hek2993 cells (Fig. 3*E*). We observed a trend where binding of *HES1* was reduced after treatment of the cells with DTT for 4 h (*p* = 0.058, paired *t* test, *n* = 5). Taken together, these results support a model where during ER stress, PERK-mediated trans-

HES1 regulates GADD34 during ER stress

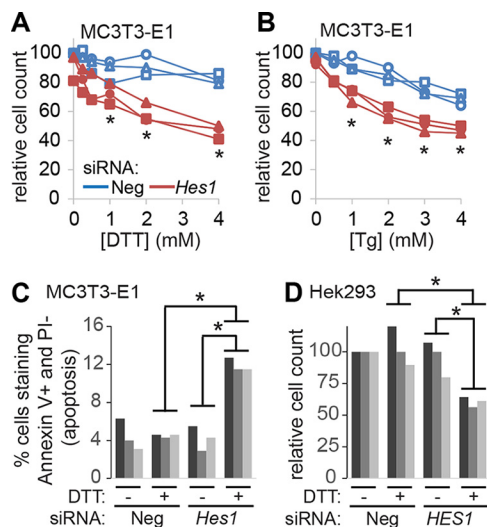


Figure 4. Knockdown of HES1 reduces cell viability in response to ER stress. A and B, we transfected MC3T3-E1 cells with either control (Neg) or *Hes1* siRNAs, incubated with various concentrations of DTT (4 h) or Tg (7 h), and counted live cells. Cell numbers were normalized to untreated Neg-control cells. C, we depleted cells of *Hes1* as in A and B, incubated with or without DTT (2 mM, 2 h), stained with Annexin V and PI, and quantified apoptosis (positive for Annexin V and negative for PI) by flow cytometry. D, we transfected Hek293 cells with either control (Neg) or *HES1* siRNAs, incubated with or without DTT (2 mM, 4 h), and counted live cells. *, p value <0.05, paired two-tailed Student's t test (in A and B, * compares Neg versus *Hes1*-depleted cells).

lational attenuation of HES1 leads to up-regulation of *HES1* mRNA through the loss of negative autoregulation.

Loss of HES1 sensitizes mammalian cells to ER stress

To characterize the role of HES1 during ER stress, we examined the viability of MC3T3-E1 cells transfected with either Neg or *Hes1* siRNAs. *Hes1* knockdown by itself did not significantly affect MC3T3-E1 cell viability in the absence of ER stressors (Fig. 4, A and B). In contrast, DTT or Tg treatment significantly compromised cell viability in a dose-dependent manner in *Hes1*-depleted cells as compared with Neg siRNA-transfected cells. To assess whether the reduced viability of *Hes1*-depleted cells during ER stress results from apoptosis, we labeled cells with Annexin V/propidium iodide (PI) and analyzed by flow cytometry. Knockdown of *Hes1* increased the percentage of cells that, after DTT treatment, were stained with Annexin V but not with PI, indicative of apoptotic signaling as opposed to necrosis (Fig. 4C). We confirmed this finding in Hek293 cells; depletion of *HES1* reduced cell viability upon DTT treatment (Fig. 4D).

HES1 regulates GADD34 during ER stress

Severe ER stress triggers cell death through expression of various pro-apoptotic genes (10). We measured the mRNA levels of several of these genes in the presence and absence of ER stress, in control and *Hes1*-depleted MC3T3-E1 cells (Fig. 5, A–E). Interestingly, expression of *Gadd34* mRNA was further increased during ER stress in cells depleted of *Hes1* (Fig. 5, A and B), consistent with a role for HES1 in repressing the transcription of *Gadd34*. This effect was conserved in human cells; *HES1*-depleted Hek293 cells showed elevated levels of *GADD34* mRNA (Fig. 5, F and G) and protein (Fig. 5, I–K). Induction of other ER stress-related pro-apoptotic genes in

mouse cells, including *Chop*, *Trib3*, and *Puma*, were not affected by *Hes1* knockdown. However, *CHOP* mRNA levels did increase with *HES1* knockdown in Hek293 cells (Fig. 5H). The difference between mouse and human cells in terms of *HES1* effects on *CHOP* expression may be explained by the presence of N-box motifs in the promoter of target genes; human *CHOP* and both mouse and human *GADD34* contain N-box motifs within 2 kb upstream of their transcription start sites, whereas mouse *Chop* does not.

To test whether HES1 directly regulates *GADD34* through repressing its transcription, we used ChIP as in Fig. 3, D and E. Endogenous HES1 protein was enriched at the *GADD34* promoter, consistent with its repressive effects on *GADD34* mRNA levels (Fig. 6). This ChIP signal did not vary significantly between untreated and DTT-treated cells, although there was a minor trend toward less binding after DTT treatment ($p = 0.085$, paired t test, $n = 5$).

Depletion of HES1 induces cell death in a GADD34-dependent manner in cells undergoing ER stress

To test whether increased expression of *GADD34* can explain the ER stress-induced cell death associated with loss of *HES1*, we compared ER stress sensitivity in cells depleted of *HES1*, *GADD34*, and both. Co-depletion of *HES1* and *GADD34* nearly completely rescued the cell death caused by depletion of *HES1* alone in both MC3T3 (Fig. 7, A–C) and Hek293 cells (Fig. 7, D–F).

GADD34 is thought to promote cell death by dephosphorylating eIF2 α , leading to the recovery of protein synthesis and potentially exacerbating ER stress if activated prematurely (16, 26). To determine whether phosphorylation of eIF2 α was affected in *HES1*-depleted cells, we compared Neg and *HES1* siRNA-transfected Hek293 cells with or without DTT for 4 h, followed by washing out the DTT and allowing cells to recover. We then measured phospho-eIF2 α (p-eIF2 α) by Western blotting (Fig. 8, A, B, and D). Total eIF2 α levels were not affected (Fig. 8C). *HES1* knockdown alone led to a small increase in p-eIF2 α levels (average 2-fold higher in *HES1*-depleted cells, p value = 0.03, $n = 3$; Fig. 8B), suggesting that loss of *HES1* causes stress at sublethal levels. However, the p-eIF2 α levels after DTT treatment were slightly lower in the *HES1* knockdown cells (average 20% lower in *HES1*-depleted cells, p value = 0.05, $n = 3$). Notably, the proportional increase in p-eIF2 α (in DTT-treated divided by untreated conditions) was lower in the *HES1*-depleted cells compared with control cells, and this trend continued throughout the recovery period (Fig. 8D). This suggests that when *HES1* is depleted, increased *GADD34* enhances dephosphorylation of eIF2 α during ER stress.

Discussion

In this study, we investigated the regulation and function of HES1 in response to ER stress. Although HES1 has not been previously identified as a regulator of ER protein folding or the secretory pathway, its mRNA levels were up-regulated by ER stress, as a result of PERK activation. We propose that translational attenuation by PERK, coupled with the documented instability of HES1 (25), leads to the initial drop in HES1 protein levels during acute ER stress (Fig. 3B). This in turn leads to a relief of transcriptional repression of its own promoter, result-

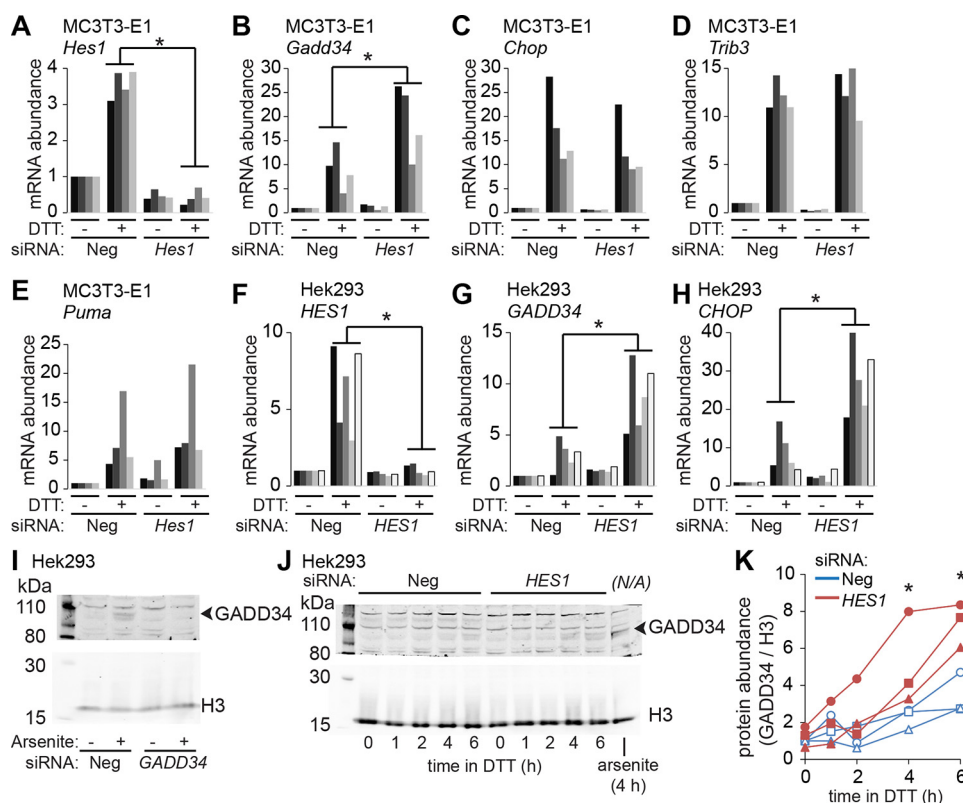


Figure 5. HES1 regulates GADD34 in response to ER stress. We measured mRNA levels of the indicated genes in MC3T3-E1 (A–E) or Hek293 (F–H) cells transfected with control (Neg) or *Hes1* siRNAs and treated with or without DTT (2 mM, 4 h). The colors of bars representing individual replicate experiments are maintained across panels A–E and F–H. I, we transfected Hek293 cells with either control (Neg) or *GADD34* siRNAs, incubated with arsenite (100 μ M, 4 h), and detected GADD34 protein by Western blotting. J and K, we depleted Hek293 cells of *HES1* as in F–H and measured GADD34 protein levels by Western blotting. Shown are a representative blot (J) and quantification from 3 independent experiments (K). *, *p* value <0.05, paired two-tailed Student’s *t* test on log₂-transformed data to test for fold-changes.

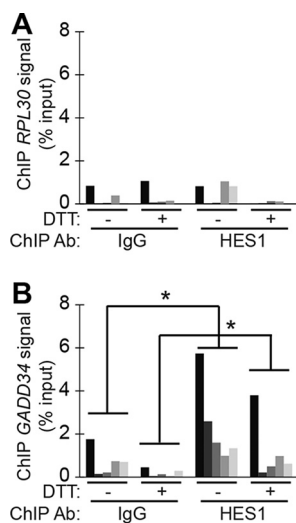


Figure 6. HES1 binds the promoter of GADD34. We used HES1 ChIP samples from Fig. 3, D and E, and measured the relative abundance of the *GADD34* promoter region in the precipitated chromatin by qPCR with *RPL30* exon3 as a negative control. Cells were untreated or treated with DTT (2 mM, 4 h) prior to ChIP. *, *p* value <0.05, paired two-tailed Student’s *t* test on log₂-transformed data to test for fold-changes.

ing in an increase in mRNA levels (Fig. 3C), followed by a rise in protein levels. Therefore, although HES1 protein levels do not typically increase above baseline levels during ER stress, this feedback regulation likely contributes to the cells’ ability to maintain the correct overall abundance of HES1.

The ability to maintain HES1 protein levels during ER stress is important, as its depletion sensitized cells to ER stress–induced apoptosis. This effect appears to be a consequence of the direct regulation of the pro-apoptotic gene *GADD34* by HES1: HES1 bound to the *GADD34* promoter, *HES1* depletion enhanced *GADD34* expression in response to ER stress, and depleting cells of *GADD34* mitigated the stress-induced apoptosis observed in *HES1*-depleted cells. *HES1* depletion also caused a 2-fold increase in eIF2 α phosphorylation in the absence of chemical inducers of ER stress, suggesting that loss of HES1 activates a mild stress response. Overall, we propose that lack of HES1 induces apoptosis during ER stress through a combination of causing low levels of stress and enhancing *GADD34*-mediated dephosphorylation of eIF2 α , thereby reversing the prosurvival effects of PERK.

Expression of *GADD34* is induced during ER stress by ATF4 and CHOP (27, 28), which are downstream targets of PERK. Because ATF4–CHOP and HES1 are each regulated by PERK but have opposite effects on *GADD34* expression, the balance and timing of these components of the UPR may be important in deciding whether cells live or die during ER stress. Interestingly, in human but not mouse cells, *HES1* depletion also led to enhanced up-regulation of *CHOP* mRNA, suggesting that HES1 represses *CHOP* transcription (Fig. 5H). This regulation would further strengthen the effects of HES1, by repressing both *GADD34* and its upstream activator simultaneously, and suppressing the pro-apoptotic effects of CHOP.

HES1 regulates GADD34 during ER stress

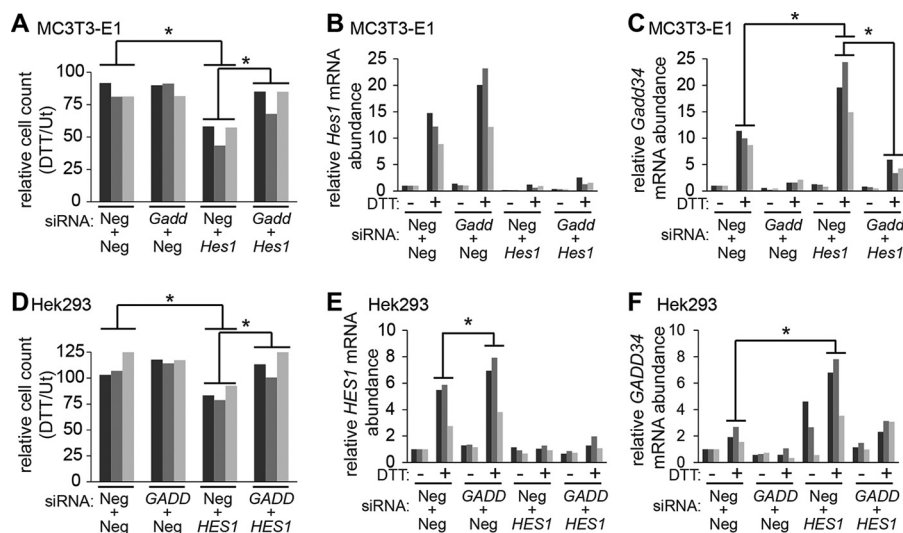


Figure 7. Stress sensitivity in cells depleted of HES1 depends on GADD34. A–F, we transfected MC3T3-E1 or Hek293 cells with Neg, HES1, GADD34, or both HES1/GADD34 siRNAs (see “Experimental procedures”) and then incubated with or without DTT (2 mM, 4 h). We then counted live cells (A and D) and measured mRNA levels of HES1 (B and E) and GADD34 (C and F) by qPCR as controls. The colors of bars representing individual replicate experiments are maintained across panels A–C and D–F. *, p value <0.05 , paired two-tailed Student’s t test on \log_2 -transformed data to test for fold-changes.

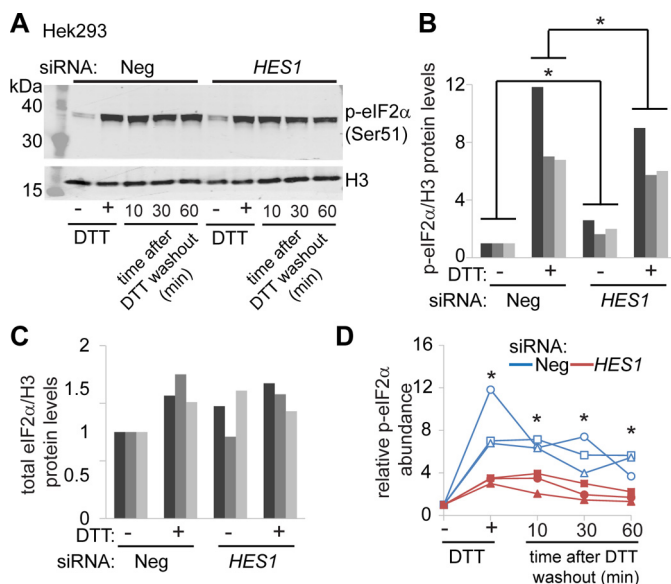


Figure 8. Depletion of HES1 affects eIF2 α phosphorylation. A, we transfected Hek293 cells with either Neg or HES1 siRNAs, incubated with or without DTT (2 mM, 4 h), washed out the DTT, and monitored phosphorylated eIF2 α (Ser⁵¹) over time by Western blotting. B and C, we quantified p-eIF2 α or total eIF2 α levels by Western blotting, from three independent experiments. The bars represent individual replicate experiments, and bars of the same color in both B and C indicate treatments done in parallel. D, we quantified p-eIF2 α levels from three independent experiments as in A, and normalized to the unstressed cells from each set of siRNA transfections. Markers of the same shape indicate treatments done in parallel. *, p value <0.05 , paired two-tailed Student’s t test on \log_2 -transformed data to test for fold-changes. Note that in B, differences between untreated and DTT-treated conditions were also statistically significant (p value <0.05).

Like HES1, the zinc finger transcription factor NMP4 has been shown to repress transcription of *GADD34* and sensitize cells to ER stress, although it represses transcription even in the absence of stress (29). HES1, in contrast, did not affect *GADD34* expression in the absence of stress (Fig. 5, B and G); HES1 may instead have a specific role in dampening the induction of *GADD34* and preventing the premature resumption of protein synthesis.

The regulation of HES1 by the UPR, and its effects on *GADD34*, may extend beyond the acute induction of ER stress studied here. For example, many components of the UPR have been implicated in cancer development (30). Cancer cells often show elevated levels of HES1 (31, 32), which is associated with poor prognosis in colorectal cancer (33, 34). It will be interesting to see whether PERK plays a role in regulation of HES1 in cancer, and whether HES1 can enhance tumor survival by repressing the expression of *GADD34* and/or *CHOP*. More broadly, because HES1 is essential for the development of some tissues where the UPR is also important (18, 35), HES1 may be targeted by the UPR or may influence UPR pathways in physiological situations.

Experimental procedures

General information, cell culture, and treatments

We cultured pre-osteoblast mouse MC3T3-E1 cells (American Type Culture Collection) in MEM α with nucleosides and no ascorbic acid (Invitrogen), and Hek293 cells in Dulbecco’s modified Eagle’s medium, both at 37 °C and 5% CO₂. We cultured *Drosophila* S2 cells (Invitrogen) in Schneider’s media at room temperature. All media were supplemented with 10% heat-inactivated fetal bovine serum. We carried out experiments at low passage numbers and did not allow cells to become confluent. To induce ER stress, we added 2 mM DTT (Sigma) or 2 μ M Tg (Sigma) to cell media. To inhibit the integrated stress response, we added 200 nM ISRIB (kind gift from the Peter Walter lab, University of California at San Francisco) to cells for ~5 min before adding ER stressors. For inhibition of translation, we treated cells with 35 μ M CHX.

RNAi

To deplete S2 cells of individual UPR transducers, we used PCR to amplify regions of cDNAs encoding *Xbp1*, *Perk*, and *Atf4*, using S2 cell cDNA as a template and primers containing T7 RNA polymerase sites on the 5’ ends. As a control, we amplified a region of the GFP coding sequence. We then used these

Table 1
List of siRNAs used in this study

Target gene	Species	siRNA	
None	None	Negative control (Qiagen, SI03650325)	
PERK	Mouse	Eif2ak3_1 (Qiagen, SI00991319)	
		Eif2ak3_3 (Qiagen, SI00991333)	
		Eif2ak3_5 (Qiagen, SI02689981)	
		Eif2ak3_6 (Qiagen, SI02736615)	
Human	Human	EIF2AK3_1 (Qiagen, SI00069048)	
		EIF2AK3_5 (Qiagen, SI02223718)	
		EIF2AK3_6 (Qiagen, SI02223725)	
		EIF2AK3_10 (Qiagen, SI04438224)	
Ire1	Mouse	Ern1_2 (Qiagen, SI00995890)	
		Ern1_4 (Qiagen, SI00995904)	
Atf4	Mouse	NM_009716 (Sigma, SASI_Mm02_00316863)	
		NM_009716 (Sigma, SASI_Mm02_00316864)	
		NM_009716 (Sigma, SASI_Mm02_00316865)	
		NM_009716 (Sigma, SASI_Mm01_00128579)	
HES1	Mouse	Hes1_5 (Qiagen, SI02667308)	
		Hes1_6 (Qiagen, SI02686992)	
		Hes1_7 (Qiagen, SI02708881)	
		Hes1_8 (Qiagen, SI02732989)	
	Human	Human	HES1_2 (Qiagen, SI00078330)
			HES1_3 (Qiagen, SI00078337)
			HES1_5 (Qiagen, SI03075016)
			HES1_5 (Qiagen, SI03075016)
GADD34	Mouse	Myd116_3 (Qiagen, SI00178241)	
		Myd116_5 (Qiagen, SI02709742)	
	Human	Human	PPP1R15A_5 (Qiagen, SI02659125)
			PPP1R15A_6 (Qiagen, SI02659132)
			PPP1R15A_8 (Qiagen, SI04439197)
			PPP1R15A_8 (Qiagen, SI04439197)

PCR products to generate dsRNA by *in vitro* transcription (Megascript T7 kit, Ambion). We incubated S2 cells with dsRNA in serum-free media for 45 min, replaced the serum, and allowed the cells to recover for 4–5 days. We then repeated the dsRNA treatment and induced ER stress 1 day following the second dsRNA treatment.

For RNAi in mammalian cells, we followed Invitrogen RNAimax guidelines for transfection of siRNAs. We combined multiple siRNAs (Qiagen) targeting each gene (Table 1). Negative siRNA-transfected cells were included as controls for all experiments. For the double knockdown experiments in Fig. 7, we used the same total amount of siRNAs (900 ng) for each treatment: single knockdowns contained either 675 ng of HES1 or 225 ng of GADD34 siRNA pools, with Neg siRNA pools making up the rest, whereas the double knockdowns contained both 675 ng of HES1 and 225 ng of GADD34 siRNA pools. We subjected cells to inhibitors and/or ER stressors 48–72 h after transfection, when cells were ~70–80% confluent.

mRNA isolation and analysis

We isolated mRNA using either TRIzol reagent (Invitrogen) or Quick RNA MiniPrep kits (Zymo Research), and synthesized cDNA using 700 ng to 2 µg of total RNA as a template, a T18 primer, and Moloney murine leukemia virus reverse transcriptase (New England Biolabs). We measured relative mRNA abundance by qPCR using the Mastercycler ep realplex (Eppendorf) with SYBR Green fluorescent dye. We measured each sample in triplicate and normalized the target mRNA levels to those of ribosomal protein (RPL19) mRNA.

We measured *Xbp1* splicing by amplifying cDNA with primers encompassing the *Xbp1* splice site and running the products on a 2% agarose gel. We then quantified the relative band intensities for the spliced and unspliced *Xbp1* products. All primer sequences are listed in Table 2.

Table 2
Primers used for qPCR and *Xbp1* splicing

Name	Sequences (5'–3')
<i>dRpl19</i>	Forward: AGGTCCGACTGCTTAGTGACC Reverse: CGCAAGCTTATCAAGGATGG
<i>hairy</i>	Forward: CGTGCCCGTATTAACAACCTG Reverse: TCTTAACGCCATTGTATGCAG
<i>dXbp1</i>	Forward: GGTATACAACAGGTGGACACA Reverse: GGGTTTCCATTATCTTCAAC
<i>dPerk</i>	Forward: CGACGACGAATTCAGCCCTAT Reverse: ACTCTTGCGGGCCGTTTCAGAT
<i>dAtf4</i>	Forward: AGACGCTGCTTCGCTTCCTTC Reverse: GCCCGTAAGTGCAGTACCGCT
<i>dNrf2</i>	Forward: GCATGGTGTGTGCCCTTCTG Reverse: ATATTTGTTGGACGACGCGAC
<i>mRpl19</i>	Forward: CTGATCAAGGATGGGCTGAT Reverse: GCCGCTATGTACAGACACGA
<i>mHes1</i>	Forward: TAACGCAGTGTACCTTCCA Reverse: AGGCGCAATCCAATATGAAC
<i>mPerk</i>	Forward: TGGACTGGTACTGCTATGG Reverse: GGTGCTGAATGGGTAGAGGA
<i>mXbp1</i>	Forward: AGAAGAGAACCACAACTCCAG Reverse: GGGTCCAATTGTCCAGAATGG
<i>mTrib3</i>	Forward: GGAACCTTCAGAGCGACTTG Reverse: CCCAAAAGTCCAGGAAAGCC
<i>mGadd34</i>	Forward: CTGCAAGGGGCTGATAAGAG Reverse: AGGGGTGACGCTTGTCTTCT
<i>mchop</i>	Forward: TATCTCATCCCCAGGAAACG Reverse: CTGCTCCTTCTCCTTCATGC
<i>mPuma</i>	Forward: GCCCAGCAGCACTTAGAGTG Reverse: TGTGATGCTGCTTCTTCTTG
<i>hRPL19</i>	Forward: ATGTATCACAGCCTGTACCTG Reverse: TTCTTGGTCTCTTCTCCTTGT
<i>hHES1</i>	Forward: CTGTATCCCCGCTTACACC Reverse: AGGCGCAATCCAATATGAAC
<i>hPERK</i>	Forward: CAGGCTTTTCCATCCTCATC Reverse: AACAACTCCAAAGCCACCAC
<i>hGADD34</i>	Forward: GAGGAGGCTGAAGACAGTGG Reverse: AATTGACTTCCCTGCCCTCT
<i>hCHOP</i>	Forward: CAGAACCAGCAGAGGTCACA Reverse: AGCTGTGCCACTTTCCTTTC
<i>hHES1 promoter</i>	Forward: GCGTGTCTCCTCCTCCATTG Reverse: GGATCCTGTGTATCCCTAGTC
<i>hGADD34 promoter</i>	Forward: CGCATTGTGATTGACAGTTCG Reverse: AAGGGTGGGAAGTGGGAAGTAA
<i>hRPL30 exon3</i>	Forward: AAAGTCGCTGGAGTTCGATCA Reverse: TACCTCAAAGCTGGGCAGTT

ChIP

We cross-linked proteins and DNA by adding formaldehyde (final concentration of 1%) to Hek293 cells and quenched 10 min later by adding glycine (final concentration 0.125 M). Cross-linked chromatin was sonicated six times at 30% power (9 s on and 1 s off) using a Branson Sonifier 450 with a microtip probe. We removed insoluble debris by centrifugation and incubated the supernatant with antibodies to HES1 (Santa Cruz Biotechnology 166410), or as a control, rabbit IgG (Cell Signaling Technology 2729), for 12 h at 4 °C. We then precipitated the immunocomplexes using ChIP-Grade Protein G Magnetic Beads (Cell Signaling Technology 9006), treated with RNase A at 37 °C for 30 min, and reversed cross-links by incubating at 65 °C for 8 h. We purified the resulting DNA using DNA Clean & Concentrator kits (Zymo Research) and analyzed by qPCR. Serial dilutions of input chromatin were used to generate stan-

HES1 regulates GADD34 during ER stress

standard curves for determining the relative amount of product, which was normalized to the input levels.

Cell viability and apoptosis assays

For viability assays in MC3T3-E1 cells, we removed floating cells by aspiration, trypsinized, and counted live cells using a hemocytometer. For Hek293 cells, which tended to release from the flasks during ER stress, we collected all cells, centrifuged (1000 × *g*, 5 min) the cells to separate dead cells (in the supernatant), resuspended cell pellets in media, and counted live cells on the hemocytometer. We used the Annexin V-Alexa Fluor 488 apoptosis assay kit (Invitrogen) to determine the percentage of apoptosis as described by the manufacturer's protocol. After staining, cells were analyzed by flow cytometry (BD Accuri C6 Flow Cytometer, BD Biosciences) and BD Accuri C6 Plus (BD Biosciences) software.

Western blotting

We lysed Hek293 cells in RIPA buffer (25 mM Tris, pH 7.6, 150 mM NaCl, 1% Nonidet P-40, 1% sodium deoxycholate, and 0.1% SDS) with protease inhibitors (Thermo Scientific) and phosphatase inhibitors (50 mM NaF and 0.2 mM sodium orthovanadate complexes). Protein concentration was determined using the Pierce BCA protein assay kit (Thermo Scientific). We added SDS loading buffer and DTT to each sample, boiled for 5 min, and resolved on 4–12% NuPAGE BisTris gels (Invitrogen). We transferred proteins to nitrocellulose membranes and probed using the following antibodies: anti-HES1 (Santa Cruz Biotechnology 25392, 1:200), anti-Histone H3 (Abcam 1791, 1:10,000), anti-Ser⁵¹-p-eIF2 α (Abcam 32157, 1:1,000), anti-eIF2 α (Abcam 26197), anti-GADD34 (Santa Cruz Biotechnology 8327, 1:400), and the secondary anti-rabbit IgG-IRDye 800CW (Licor 926–32210, 1:10,000). We scanned the blots and quantified band intensities using a Licor Odyssey imager. Protein levels for each sample were divided by histone H3 levels measured in the same blot. Bands for HES1 and GADD34 were confirmed by using RNAi to deplete cells of these proteins (Figs. 3A and 5I) and by treating cells with arsenite (100 μ M, 4 h) as a positive control for increasing GADD34 protein levels (Fig. 5, I and J).

Data presentation

We displayed all data for individual experiments. In bar graphs, experimental treatments done in parallel are correlated by color, and when appropriate these colors are consistent across panels (for example, when different mRNAs are measured in the same samples, the replicates are color-coded across panels and noted in the figure legends). In scatterplots, experimental treatments done in parallel are correlated by symbol and connected by lines. Statistical significance for all expression data were determined using paired two-tailed Student's *t* tests on log₂-transformed data to test for fold-changes.

Author contributions—J. E. L., W. M., and J. H. conceptualization; J. E. L., W. M., and J. H. formal analysis; J. E. L., W. M., and J. H. investigation; J. E. L. and J. H. methodology; J. E. L., W. M., and J. H. writing-original draft; J. E. L. and J. H. writing-review and editing; J. H. funding acquisition; J. H. project administration.

Acknowledgments—We thank McKenna Oney for assistance with RNAi in S2 cells, Jess Mella for assistance with post-review experiments, and members of the Hollien lab for discussions and critical reading of the manuscript. We also thank Bradley Cairns and Chongli Yi for technical advice and use of equipment for ChIP.

References

1. Walter, P., and Ron, D. (2011) The unfolded protein response: from stress pathway to homeostatic regulation. *Science* **334**, 1081–1086 [CrossRef](#) [Medline](#)
2. Harding, H. P., Zhang, Y., and Ron, D. (1999) Protein translation and folding are coupled by an endoplasmic-reticulum-resident kinase. *Nature* **397**, 271–274 [CrossRef](#) [Medline](#)
3. Hollien, J., and Weissman, J. S. (2006) Decay of endoplasmic reticulum-localized mRNAs during the unfolded protein response. *Science* **313**, 104–107 [CrossRef](#) [Medline](#)
4. Vattem, K. M., and Wek, R. C. (2004) Reinitiation involving upstream ORFs regulates ATF4 mRNA translation in mammalian cells. *Proc. Natl. Acad. Sci. U.S.A.* **101**, 11269–11274 [CrossRef](#) [Medline](#)
5. Harding, H. P., Zhang, Y., Zeng, H., Novoa, I., Lu, P. D., Calton, M., Sadri, N., Yun, C., Popko, B., Paules, R., Stojdl, D. F., Bell, J. C., Hettmann, T., Leiden, J. M., and Ron, D. (2003) An integrated stress response regulates amino acid metabolism and resistance to oxidative stress. *Mol. Cell* **11**, 619–633 [CrossRef](#) [Medline](#)
6. Calton, M., Zeng, H., Urano, F., Till, J. H., Hubbard, S. R., Harding, H. P., Clark, S. G., and Ron, D. (2002) IRE1 couples endoplasmic reticulum load to secretory capacity by processing the XBP-1 mRNA. *Nature* **415**, 92–96 [CrossRef](#) [Medline](#)
7. Yoshida, H., Matsui, T., Yamamoto, A., Okada, T., and Mori, K. (2001) XBP1 mRNA is induced by ATF6 and spliced by IRE1 in response to ER stress to produce a highly active transcription factor. *Cell* **107**, 881–891 [CrossRef](#) [Medline](#)
8. Hollien, J., Lin, J. H., Li, H., Stevens, N., Walter, P., and Weissman, J. S. (2009) Regulated Ire1-dependent decay of messenger RNAs in mammalian cells. *J. Cell Biol.* **186**, 323–331 [CrossRef](#)
9. Yamamoto, K., Sato, T., Matsui, T., Sato, M., Okada, T., Yoshida, H., Harada, A., and Mori, K. (2007) Transcriptional induction of mammalian ER quality control proteins is mediated by single or combined action of ATF6 α and XBP1. *Dev. Cell.* **13**, 365–376 [CrossRef](#) [Medline](#)
10. Tabas, I., and Ron, D. (2011) Integrating the mechanisms of apoptosis induced by endoplasmic reticulum stress. *Nat. Cell Biol.* **13**, 184–190 [CrossRef](#) [Medline](#)
11. Urano, F., Wang, X., Bertolotti, A., Zhang, Y., Chung, P., Harding, H. P., and Ron, D. (2000) Coupling of stress in the ER to activation of JNK protein kinases by transmembrane protein kinase IRE1. *Science* **287**, 664–666 [CrossRef](#) [Medline](#)
12. Xia, Z., Dickens, M., Raingeaud, J., Davis, R. J., and Greenberg, M. E. (1995) Opposing effects of ERK and JNK-p38 MAP kinases on apoptosis. *Science* **270**, 1326–1331 [CrossRef](#) [Medline](#)
13. Li, B., Yi, P., Zhang, B., Xu, C., Liu, Q., Pi, Z., Xu, X., Chevet, E., and Liu, J. (2011) Differences in endoplasmic reticulum stress signalling kinetics determine cell survival outcome through activation of MKP-1. *Cell. Signal.* **23**, 35–45 [CrossRef](#) [Medline](#)
14. Zinszner, H., Kuroda, M., Wang, X., Batchvarova, N., Lightfoot, R. T., Remotti, H., Stevens, J. L., and Ron, D. (1998) CHOP is implicated in programmed cell death in response to impaired function of the endoplasmic reticulum. *Genes Dev.* **12**, 982–995 [CrossRef](#) [Medline](#)
15. Szegezdi, E., Logue, S. E., Gorman, A. M., and Samali, A. (2006) Mediators of endoplasmic reticulum stress-induced apoptosis. *EMBO Rep.* **7**, 880–885 [CrossRef](#) [Medline](#)
16. Novoa, I., Zeng, H., Harding, H. P., and Ron, D. (2001) Feedback inhibition of the unfolded protein response by GADD34-mediated dephosphorylation of eIF2 α . *J. Cell Biol.* **153**, 1011–1022 [CrossRef](#)

17. Kageyama, R., Ohtsuka, T., and Tomita, K. (2000) The bHLH gene Hes1 regulates differentiation of multiple cell types. *Mol. Cells* **10**, 1–7 [CrossRef Medline](#)
18. Kobayashi, T., and Kageyama, R. (2014) Expression dynamics and functions of Hes factors in development and diseases. *Curr. Top. Dev. Biol.* **110**, 263–283 [CrossRef Medline](#)
19. Szabat, M., Kalynyak, T. B., Lim, G. E., Chu, K. Y., Yang, Y. H., Asadi, A., Gage, B. K., Ao, Z., Warnock, G. L., Piret, J. M., Kieffer, T. J., and Johnson, J. D. (2011) Musashi expression in β -cells coordinates insulin expression, apoptosis and proliferation in response to endoplasmic reticulum stress in diabetes. *Cell Death Dis.* **2**, e232 [CrossRef Medline](#)
20. Cullinan, S. B., Zhang, D., Hannink, M., Arvisais, E., Kaufman, R. J., and Diehl, J. A. (2003) Nrf2 is a direct PERK substrate and effector of PERK-dependent cell survival. *Mol. Cell. Biol.* **23**, 7198–7209 [CrossRef Medline](#)
21. Bobrovnikova-Marjon, E., Pytel, D., Riese, M. J., Vaites, L. P., Singh, N., Koretzky, G. A., Witze, E. S., and Diehl, J. A. (2012) PERK utilizes intrinsic lipid kinase activity to generate phosphatidic acid, mediate Akt activation, and promote adipocyte differentiation. *Mol. Cell. Biol.* **32**, 2268–2278 [CrossRef Medline](#)
22. Zhang, W., Hietakangas, V., Wee, S., Lim, S. C., Gunaratne, J., and Cohen, S. M. (2013) ER stress potentiates insulin resistance through PERK-mediated FOXO phosphorylation. *Genes Dev.* **27**, 441–449 [CrossRef Medline](#)
23. Sidrauski, C., Acosta-Alvear, D., Khoutorsky, A., Vedantham, P., Hearn, B. R., Li, H., Gamache, K., Gallagher, C. M., Ang, K. K., Wilson, C., Okreglak, V., Ashkenazi, A., Hann, B., Nader, K., Arkin, M. R., Renslo, A. R., Sonenberg, N., and Walter, P. (2013) Pharmacological brake-release of mRNA translation enhances cognitive memory. *Elife* **2**, e00498 [Medline](#)
24. Takebayashi, K., Sasai, Y., Sakai, Y., Watanabe, T., Nakanishi, S., and Kageyama, R. (1994) Structure, chromosomal locus, and promoter analysis of the gene encoding the mouse helix-loop-helix factor HES-1: negative autoregulation through the multiple N box elements. *J. Biol. Chem.* **269**, 5150–5156 [Medline](#)
25. Hirata, H., Yoshiura, S., Ohtsuka, T., Bessho, Y., Harada, T., Yoshikawa, K., and Kageyama, R. (2002) Oscillatory expression of the bHLH factor Hes1 regulated by a negative feedback loop. *Science* **298**, 840–843 [CrossRef Medline](#)
26. Novoa, I., Zhang, Y., Zeng, H., Jungreis, R., Harding, H. P., and Ron, D. (2003) Stress-induced gene expression requires programmed recovery from translational repression. *EMBO J.* **22**, 1180–1187 [CrossRef Medline](#)
27. Ma, Y., and Hendershot, L. M. (2003) Delineation of a negative feedback regulatory loop that controls protein translation during endoplasmic reticulum stress. *J. Biol. Chem.* **278**, 34864–34873 [CrossRef Medline](#)
28. Marciniak, S. J., Yun, C. Y., Oyadomari, S., Novoa, I., Zhang, Y., Jungreis, R., Nagata, K., Harding, H. P., and Ron, D. (2004) CHOP induces death by promoting protein synthesis and oxidation in the stressed endoplasmic reticulum. *Genes Dev.* **18**, 3066–3077 [CrossRef Medline](#)
29. Young, S. K., Shao, Y., Bidwell, J. P., and Wek, R. C. (2016) Nuclear matrix protein 4 is a novel regulator of ribosome biogenesis and controls the unfolded protein response via repression of Gadd34 expression. *J. Biol. Chem.* **291**, 13780–13788 [CrossRef Medline](#)
30. Ma, Y., and Hendershot, L. M. (2004) The role of the unfolded protein response in tumour development: friend or foe? *Nat. Rev. Cancer* **4**, 966–977 [CrossRef Medline](#)
31. Wang, X., Fu, Y., Chen, X., Ye, J., Lü, B., Ye, F., Lü, W., and Xie, X. (2010) The expressions of bHLH gene HES1 and HES5 in advanced ovarian serous adenocarcinomas and their prognostic significance: a retrospective clinical study. *J. Cancer Res. Clin. Oncol.* **136**, 989–996 [CrossRef Medline](#)
32. Gao, F., Zhang, Y., Wang, S., Liu, Y., Zheng, L., Yang, J., Huang, W., Ye, Y., Luo, W., and Xiao, D. (2014) Hes1 is involved in the self-renewal and tumorigenicity of stem-like cancer cells in colon cancer. *Sci. Rep.* **4**, 3963 [Medline](#)
33. Weng, M. T., Tsao, P. N., Lin, H. L., Tung, C. C., Change, M. C., Chang, Y. T., Wong, J. M., and Wei, S. C. (2015) Hes1 increases the invasion ability of colorectal cancer cells via the STAT3-MMP14 pathway. *PLoS ONE* **10**, e0144322 [CrossRef Medline](#)
34. Yuan, R., Ke, J., Sun, L., He, Z., Zou, Y., He, X., Chen, Y., Wu, X., Cai, Z., Wang, L., Wang, J., Fan, X., Wu, X., and Lan, P. (2015) HES1 promotes metastasis and predicts poor survival in patients with colorectal cancer. *Clin. Exp. Metastasis.* **32**, 169–179 [CrossRef Medline](#)
35. Moore, K. A., and Hollien, J. (2012) The unfolded protein response in secretory cell function. *Annu. Rev. Genet.* **46**, 165–183 [CrossRef Medline](#)